AIP ADVANCES **6**, 055312 (2016)

Study on the electromagnetic waves propagation characteristics in partially ionized plasma slabs

Zhi-Bin Wang,[1,2,a] Bo-Wen Li,[1] Qiu-Yue Nie,[2,3] Xiao-Gang Wang,[1,2] and Fan-Rong Kong[3]
[1]*Department of Physics, Harbin Institute of Technology, Harbin 150001, China*
[2]*Laboratory for Space Environment and Physical Sciences, Harbin Institute of Technology, Harbin 150001, China*
[3]*School of Electrical Engineering and Automation, Harbin Institute of Technology, Harbin 150001, China*

(Received 24 March 2016; accepted 4 May 2016; published online 11 May 2016)

Propagation characteristics of electromagnetic (EM) waves in partially ionized plasma slabs are studied in this paper. Such features are significant to applications in plasma antennas, blackout of re-entry flying vehicles, wave energy injection to plasmas, and etc. We in this paper developed a theoretical model of EM wave propagation perpendicular to a plasma slab with a one-dimensional density inhomogeneity along propagation direction to investigate essential characteristics of EM wave propagation in nonuniform plasmas. Particularly, the EM wave propagation in sub-wavelength plasma slabs, where the geometric optics approximation fails, is studied and in comparison with thicker slabs where the geometric optics approximation applies. The influences of both plasma and collisional frequencies, as well as the width of the plasma slab, on the EM wave propagation characteristics are discussed. The results can help the further understanding of propagation behaviours of EM waves in nonuniform plasma, and applications of the interactions between EM waves and plasmas. [http://dx.doi.org/10.1063/1.4950772]

I. INTRODUCTION

Partially ionized plasma layers are commonly formed in many artificially applied or naturally generated processes, such as plasma antennas, reentry plasma sheaths of spacecraft, and etc.[1,2] Characterized by non-uniformity of plasma distributions, a high number density of neutral particles, a broad frequency range of electron-neutral collisions, the partially ionized plasma slabs have been studied extensively, for radio-frequency (rf) wave communication and control, material processing, and other applications.[3–10] Especially, the interaction between partially ionized plasmas and electromagnetic (EM) waves becomes a key issue not only in the fundamental studies, but also in the practical applications.[11–13] Take communication and control during spacecraft reentry for example, as to the case with a highly nonuniform plasma layer covering the vehicle, understanding of the interaction between EM waves and such typical plasmas is crucial to performance reliable communication, and extensively investigated. For example, Swift and Evans studied the propagation characteristics of the planar EM waves in inhomogeneous plasmas by a numerical integration method.[14] Gregoire *et al*. derived the basic formula of electromagnetic wave propagation in non-magnetized plasmas.[15] M. Laroussi studied the refractive index, attenuation coefficient, skin depth and phase coefficient of microwaves by a nonuniform atmospheric pressure plasma slab, and their functional dependence on the plasma density, electromagnetic wave frequency and incidence angle is discussed.[16–18] It was then found that the EM waves were greatly influenced by the plasma number density, the collisional frequency, and the electron distributions in the plasma slabs.

[a]Corresponding author: wangzhibin@hit.edu.cn

Nevertheless, the width of blackout plasma sheaths covering the flying vehicle is usually on the same order of or even shorter than the wavelength of rf waves applied. In this case then, the rf EM waves propagate in a sub-wavelength regime, where the propagation characteristics should be significantly different from that in the geometric optics regime.[19] Thus, WKB methods used previously for EM wave propagations in plasma layers[20,21] are not applicable for such cases. On the other hand, many earlier studies on plasma layers simply treated them as constant dielectric media,[22–25] and thus inhomogeneity of the plasma distribution was ignored. However, the actual plasma layers are not only dispersive, but also highly nonuniform and even highly dissipative, much more complicated than the uniform dielectric medium.[26]

Guided by previous researches and taking the sub-wavelength property into account, we in this paper develop a physical model and corresponding differential thin layer method to investigate the EM wave propagation characteristics in nonuniform sub-wavelength plasma slabs with a broad range of collision frequencies. The results will be helpful for deep understanding of the interaction behaviors between EM waves and the nonuniform plasma slabs.

The layout of the paper is as follows. The model is described in Sec. II, and the numerical results are shown in the section followed. With further discussions, the paper is then summarized in Sec. IV by concluding remarks.

II. MODELING DESCRIPTION

To focus on essential features of EM wave propagation in a thin layer of the partially ionized and unmagnetized plasma, and based on the fact that the width of the thin layer is much less than the length scale in the other directions, we in this paper use a plasma slab model, extending infinitely on the (y, z)-plane and varying only in the x-direction with a width of d. The incident EM wave also propagates in the x-direction, i.e., $\mathbf{k} = k\hat{x}$, to simplify the problem to a one-dimensional (1D) model, and polarizes in the y-direction to make it a planar wave. The equations of EM fields can be written as

$$\frac{\partial \mathbf{B}}{\partial t} = -c\nabla \times \mathbf{E}, \tag{1}$$

$$c\nabla \times \mathbf{B} = 4\pi \mathbf{J} + \frac{\partial \mathbf{E}}{\partial t}, \tag{2}$$

to get

$$-\nabla \times (\nabla \times \mathbf{E}) = \frac{4\pi}{c^2}\frac{\partial \mathbf{J}}{\partial t} + \frac{1}{c^2}\frac{\partial^2 \mathbf{E}}{\partial t^2}. \tag{3}$$

The equation for the electron motion in the unmagnetized and partially ionized plasma in the linear wave approximation has a form of

$$n_e m_e \frac{\partial \mathbf{u}_e}{\partial t} \approx -n_e e\mathbf{E} - \nu_{en} n_e m_e \mathbf{u}_e. \tag{4}$$

where the last term on the right-hand-side (RHS) of (4) is caused heavily electron- neutral collisions in the partially ionized plasma with ν_{en} is the corresponding collision frequency. The current density can then be obtained as

$$\mathbf{J} = n_i e\mathbf{u}_i - n_e e\mathbf{u}_e \approx -n_e e\mathbf{u}_e. \tag{5}$$

Substituting (4) into (5), we get

$$\begin{aligned}\frac{4\pi}{c^2}\frac{\partial \mathbf{J}}{\partial t} &\approx -\frac{4\pi n_e e}{c^2}\frac{\partial \mathbf{u}_e}{\partial t} = \frac{\omega_{pe}^2}{c^2}\mathbf{E} - \frac{4\pi\nu_{en}}{c^2}\mathbf{J} \\ &\approx \frac{\omega_{pe}^2}{c^2}\left(1 - \frac{i\nu_{en}}{\omega_0 + i\nu_{en}}\right)\mathbf{E} = \frac{\omega_{pe}^2}{c^2}\frac{\omega_0}{\omega_0 + i\nu_{en}}\mathbf{E},\end{aligned} \tag{6}$$

$$\nabla \times (\nabla \times \mathbf{E}) + \frac{1}{c^2}\frac{\partial^2 \mathbf{E}}{\partial t^2} + \frac{\omega_{pe}^2}{c^2}\frac{\omega_0}{\omega_0 + i\nu_{en}}\mathbf{E} = 0. \tag{7}$$

where ω_0 is the angular frequency of the incident EM wave, and the plasma frequency $\omega_{pe} = (4\pi n_e e^2/m_e)^{1/2}$.

To solve the equations, we represent the EM wave as $\mathbf{E}(x,t) = \hat{y}\bar{E}(x,t)e^{-i\omega_0 t}$, where $\bar{E}(x,t)$ is the amplitude of the EM wave varying slowly with time due to the dissipation and damping effects when propagating in the plasma. Because of the slowly temporal variation, the high order time derivative terms are neglected. Thus we can obtain

$$\left[i\frac{\partial}{\partial\tau} + \frac{\partial^2}{2\partial\xi^2} + \frac{1}{2}\left(1 - \frac{\tilde{n}_e(\xi)}{1 + i\tilde{\nu}_{en}}\right)\right]\bar{E}(\xi,\tau) = 0, \tag{8}$$

where the normalized spatial and temporal variables $\tau = \omega_0 t$ and $\xi = k_0 x = \omega_0 x/c$ respectively, $\tilde{\nu}_{en} \equiv \nu_{en}/\omega_0$, and $\tilde{n}_e(\xi) \equiv n_e(\xi)/n_c = \tilde{\omega}_{pe}^2 \equiv (\omega_{pe}/\omega_0)^2$ is the critical density of the plasma, with $n_c = m_e\omega_0^2/4\pi e^2$. Eq. (8) is a normalized Schrödinger equation, and its property can be a subject of other works. We in this paper however concentrate only on its steady state solution. Then the steady-state equation is written

$$\left[\frac{d^2}{d\xi^2} + \left(1 - \frac{\tilde{n}_e(\xi)}{1 + i\tilde{\nu}_{en}}\right)\right]\bar{E}(\xi) = 0 \tag{9}$$

In the geometrical optics regime, we can apply the WKB method to easily solve Eq. (9). In the sub-wavelength regime, however, the WKB approximation is not valid anymore. One then has to solve the equation by directly integrating it along ξ to get a full wave solution. However, to simplify the process, we in this paper introduce a differential thin layer method to solve Eq. (9).

Dividing the plasma slab into a number of thin layer that is much thinner than the wavelength of the incident EM wave, λ, and the typical length scale of the plasma, say, $L_n = \tilde{n}_e/(\partial\tilde{n}_e/\partial\xi)$, then in the m-th layer, $\tilde{n}_e(\xi) \approx \tilde{n}_e(\xi_m) = const.$, and

$$\bar{E}(\xi_{m+1}) \approx \bar{E}(\xi_m)e^{iN(\xi_m)\xi_m} = \bar{E}(0)e^{i\phi}\prod_{l=0}^{m} e^{iN(\xi_l)\xi_l} \tag{10}$$

where, $N(\xi) \equiv k + iK$, and ϕ is the initial phase of the EM wave at $\xi = 0$. We thus derive

$$N^2(\xi) \equiv 1 - \frac{\tilde{n}_e(\xi)}{1 + i\tilde{\nu}_{en}} = 1 - \frac{\tilde{n}_e(\xi)}{1 + \tilde{\nu}_{en}^2} + i\frac{\tilde{n}_e(\xi)\tilde{\nu}_{en}}{1 + \tilde{\nu}_{en}^2} \equiv A + iB \tag{11}$$

$$\begin{aligned} k(\xi) &= \frac{1}{\sqrt{2}}\left[\left(A^2 + B^2\right)^{1/2} + A\right]^{1/2} \\ &= \frac{1}{\sqrt{2}}\left[\left(\left(1 - \frac{\tilde{n}_e(\xi)}{1 + \tilde{\nu}_{en}^2}\right)^2 + \left(\frac{\tilde{n}_e(\xi)\tilde{\nu}_{en}}{1 + \tilde{\nu}_{en}^2}\right)^2\right)^{1/2} + \left(1 - \frac{\tilde{n}_e(\xi)}{1 + \tilde{\nu}_{en}^2}\right)\right]^{1/2}, \end{aligned} \tag{12}$$

$$\begin{aligned} K(\xi) &= \frac{1}{\sqrt{2}}\left[\left(A^2 + B^2\right)^{1/2} - A\right]^{1/2} \\ &= \frac{1}{\sqrt{2}}\left[\left(\left(1 - \frac{\tilde{n}_e(\xi)}{1 + \tilde{\nu}_{en}^2}\right)^2 + \left(\frac{\tilde{n}_e(\xi)\tilde{\nu}_{en}}{1 + \tilde{\nu}_{en}^2}\right)^2\right)^{1/2} - \left(1 - \frac{\tilde{n}_e(\xi)}{1 + \tilde{\nu}_{en}^2}\right)\right]^{1/2}, \end{aligned} \tag{13}$$

with $k(\xi)$ represents the propagation and $K(\xi)$ represents the dumping.

To make the solution converged, we take the number of layers used in this study as 150 and the corresponding layer width is then $d/150$. Convergence study is taken and the relative error of the simulation results is calculated. It is found that the relative error decays exponentially as the number of differential thin layers rises. For the layer number reaches 150, the error is calculated less than 1%.

The typical profile shape of the plasma number density applied in this paper is shown in Fig. 1, where the width of the plasma slab, $d = 5\lambda$, is used as an example. The plasma density in such profiles increases parabolicly from zero to the maximum n_0 at the middle width of the slab, and then remains constant. The corresponding plasma frequency at the flatten top is written

$$\tilde{\omega}_{pe0} = \tilde{\omega}_{pe,MAX} = (n_0/n_c)^{1/2} \equiv \tilde{n}_0^{1/2}. \tag{14}$$

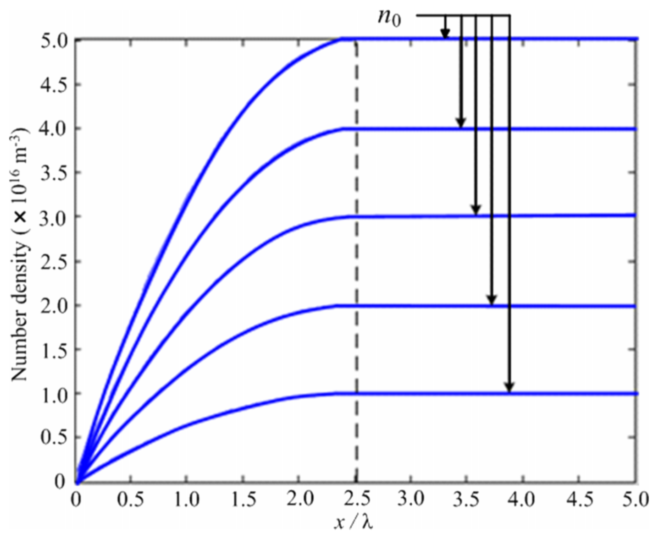

FIG. 1. Diagram of the typical plasma number density profiles.

III. RESULTS AND DISCUSSIONS

In the sub-wavelength regime interested, the width of the slab is on the order of the EM wavelength scale or thinner, thus geometrical optics approximation is not applicable. Fortunately, the physical model established in this paper can be used for both sub-wavelength and geometrical optics regimes. Based on the model described above, the overall distribution of the amplitude of the EM wave (A_{EM}) can be obtained, where A_{EM} is normalized by the initial EM wave amplitude (A_0).

Similar to the tunnel effect in quantum mechanics, an EM wave penetrates a sub-wavelength plasma layer has both theoretical significance and substantial applications in rf communications, blackout mitigation, and nano-scale optics of visible lights. Figure 2 shows an example of the amplitude of the EM wave changing with both $\tilde{\omega}_{pe0}$ and $\tilde{\nu}_{en}$ in two typical widths of the plasma slabs (d = 0.5λ and d = 2λ). It can be seen from the figure that the overall wave amplitude distribution in the plasma slabs with different widths are similar. However, the minimal amplitude of the EM wave decreases obviously with increasing the width of the plasma slabs. If $A_{\mathrm{EM}} > 1/\mathrm{e}$ (e ≈ 2.718) is applied as a criterion for the effective penetration of the EM wave into the plasma slabs, Fig. 2 shows that the EM wave effectively penetrates the slab for all parameter domain of $\tilde{\omega}_{pe0}$ and $\tilde{\nu}_{en}$, enclosed by the bold black dash lines in Fig 2(c) for the thinner slab of d = 0.5λ. On the other hand, to the thicker slab of d = 2λ, the domain bounded by the bold black dash lines in Fig. 2(d) is smaller.

We then study the wave penetration into the plasma slab in details for specific cases. To show the penetration, the amplitude of the EM wave (A_{EM}) in the plasma slab ($d = 5\lambda$) in different collision regimes, with $\tilde{\nu}_{en} = 0.001$ in (a) and $\tilde{\nu}_{en} = 1.8$ in (b), is presented in Figure 3. In the weak collision regime of Fig. 3(a), as indicated in Fig 2, the turning point of the A_{EM} curve is near the critical point of $x = x_c$ where $\tilde{\omega}_{pe} = 1$, i.e., the plasma number density is equal to the critical density n_c. After the turning point, A_{EM} decreases sharply as the plasma number density gets over n_c. Nevertheless, in the strong collision regime of Fig. 3(b), the wave amplitude A_{EM} varies smoothly without a clear turning point.

We then further discuss the effect of crucial parameters of $\tilde{\omega}_{pe0}$ and $\tilde{\nu}_{en}$. The influence of the normalized collisional frequency ($\tilde{\omega}_{pe0}$) on the amplitude of the EM wave (A_{EM}), with several typical normalized plasma frequencies ($\tilde{\nu}_{en}$), is shown in Fig. 4(a). On the other hand, the influence of the normalized collisional frequency ($\tilde{\nu}_{en}$) on the amplitude of the EM wave (A_{EM}), with several typical normalized plasma frequencies ($\tilde{\omega}_{pe0}$), is seen in Fig. 4(b). It is revealed in Fig. 4(a) that in the regime of weak collision, A_{EM} falls rapidly when the normalized plasma frequency ($\tilde{\omega}_{pe0}$) is greater than 1, i.e., in the flatten region the plasma is dense, $n_0 > n_c$. And the weaker the collision frequency is, the sharper A_{EM} falls in this dense regime. On the other hand, in the strongly

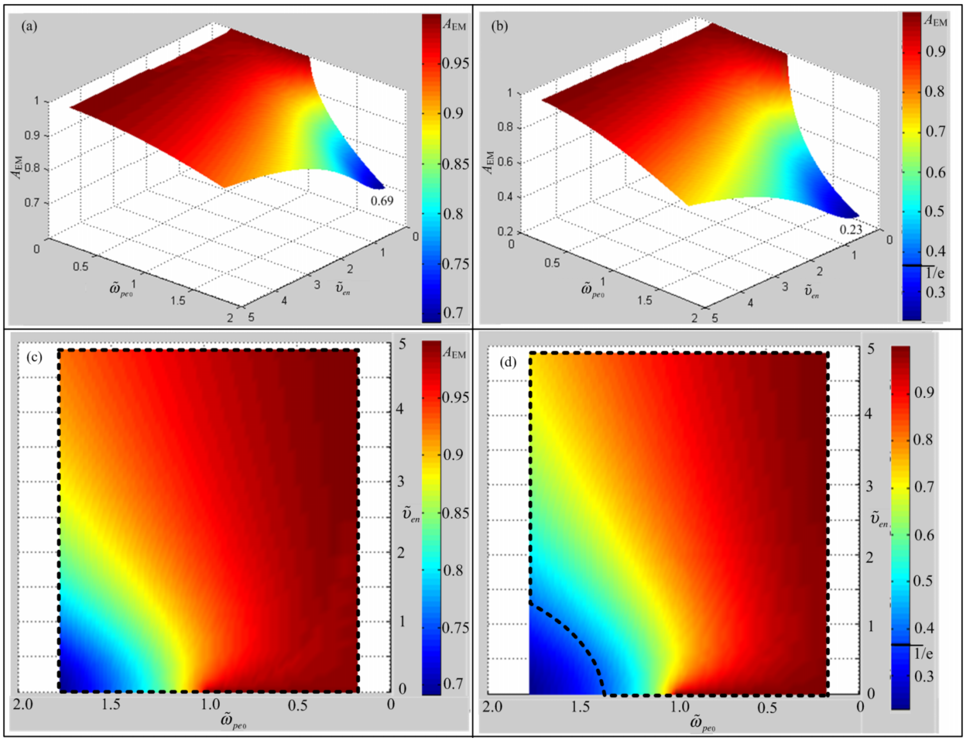

FIG. 2. The amplitude of the EM wave (A_{EM}) vs. $\tilde{\omega}_{pe0}$ and $\tilde{\nu}_{en}$ with (a) and (c) for d=0.5λ, and (b) and (d) for $d = 2\lambda$; in (c) and (d), the penetration regime is bounded by the dash lines.

collisional regime, the EM wave amplitude (A_{EM}) decreases gradually as the normalized plasma frequency ($\tilde{\omega}_{pe0}$) rises. Nevertheless A_{EM} is still notable even if the normalized plasma frequency ($\tilde{\omega}_{pe0}$) reaches a level as high as 1.8, i.e., the plasma is overdense. Figure 4(b) shows that in the dense regimeA_{EM} varies monotonously as the collision gets stronger ($\tilde{\omega}_{pe0} > 1$, $n_0 > n_c$), but nonmonotonously in the low-density regime ($\tilde{\omega}_{pe0} < 1$, $n_0 < n_c$). However, in both regimes, A_{EM} increases with $\tilde{\nu}_{en}$ monotonically when $\tilde{\nu}_{en} > 1$. In other words, the strong collision ($\tilde{\nu}_{en} > 1$) helps the transmission of the EM wave in the sub-wavelength plasma slab. It can be understood by the propagation property of the wave, the wavevector, of which the magnitude $k = k(\xi)$ is given by Eq. (12). In the parameter regime of Fig. 4(b), clearly $k = k(\xi)$ is monotonously rises with the collision frequency.

The effect of the density profile shape on the propagation feature of EM waves is further investigated in Fig. 5.

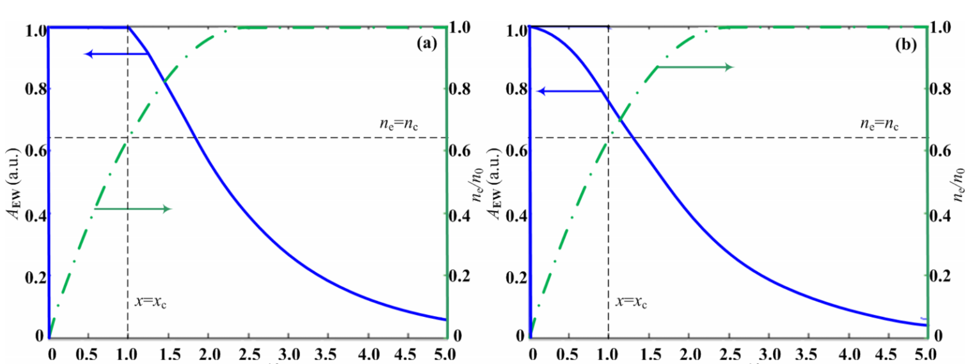

FIG. 3. The wave amplitude in various plasma slabs of different collision regimes, with (a) $\tilde{\nu}_{en} = 0.001$, and (b) $\tilde{\nu}_{en} = 1.8$.

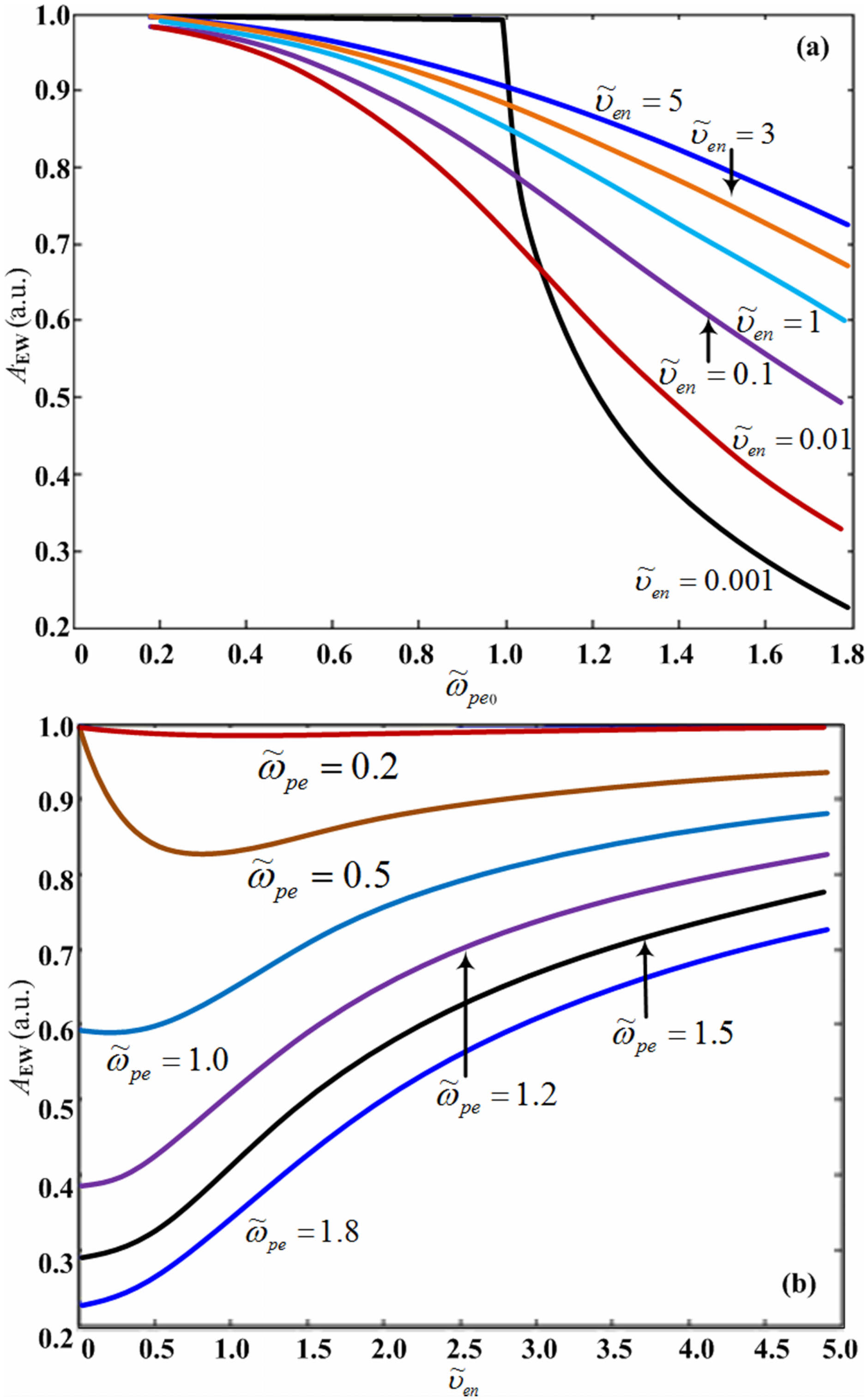

FIG. 4. Representative cases of the wave amplitude (A_{EM}) vs. (a) $\hat{\omega}_{pe}$, and (b) $\tilde{\nu}_{en}$.

In Fig. 5(a) the plasma density ramps up from zero to $n_0 > n_c$ parabolicly. And in 5(b) and 5(c), it rises to $n_0 > n_c$ and $n_0 = n_c$ respectively and remains at the level to form a flatten region. In Fig. 5(d) and 5(e) however, the plasma density profile is parabolicly symmetric about its center $x = 0.5d$ with a maximum of $n_0 > n_c$ and $n_0 = n_c$ respectively. Thus, there are two profiles with

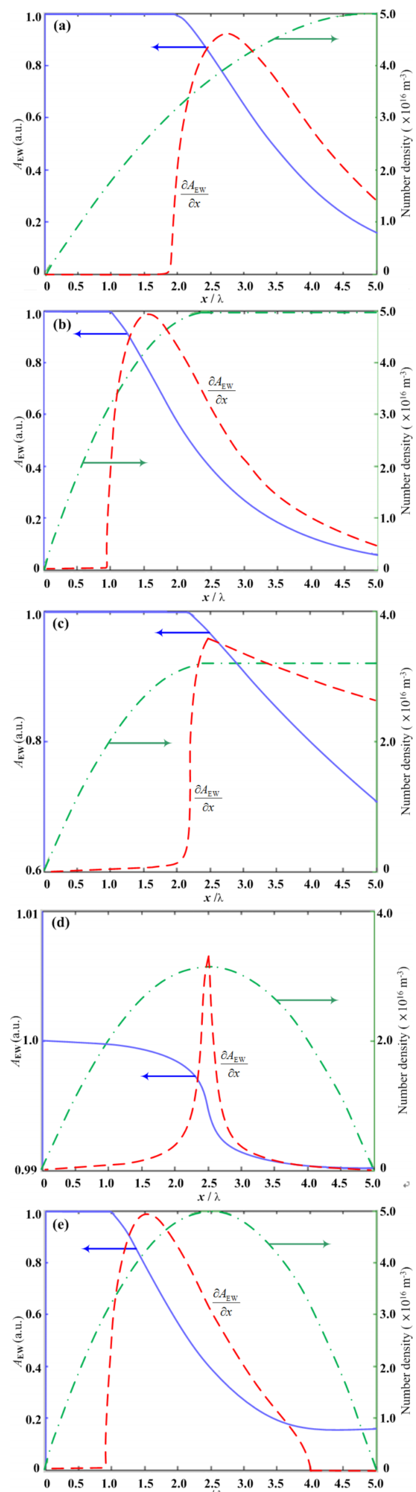

FIG. 5. The variation of A_{EM} for different plasma profiles in the weak collision regime.

a dense region, two profiles with a critical region (one of them is a point), and a low density profile. The dash dot curve (green) describes the profile shapes, and the solid (blue) shows the wave amplitude A_{EM} as propagating into the plasma slabs, while the dashed (red) is the spatial variation of A_{EM}, $\partial A_{EM}/\partial x$. It is found that, in the weak collision regime with $\tilde{\nu}_{en} = 0.001$, A_{EM} decreases sharply as the plasma density goes beyond n_c, no matter in which kind of the plasma profile type. If the maximum plasma number density (n_0) is equal to n_c, the maximum reflection/absorption is located at the critical point. However, if the maximum plasma number density (n_0) is higher than n_c, the maximum reflection/absorption is moved to a higher density spot between the critical point and where the plasma number density just reaches n_0. For the density profile discussed in this paper with a ramp at the EM wave incident side, the wave is not reflected directly without getting into the plasma slab. In fact, even in the weak collision regime, the EM wave is able to get into the overdense plasma slab in a scale on the order of the skin depth ($\sim c/\omega_{pe0}$), and then reflected if d is much thicker than the skin depth. By the penetrated wave energy, one can calculate the energy reflection and absorption.

IV. CONCLUDING REMARKS

The propagation characteristics of EM waves propagating vertically to a partially ionized nonuniform plasma slab are investigated by a theoretical model solved by a differential thin layer method numerically in this paper. The influences of the plasma and the collision frequencies on the amplitudes of the EM waves are discussed, for plasma slabs with various shapes and width of the density profile. The main results are as follows:

(1) For plasma slabs with different widths but similar profile shapes of the density distribution, the minimal amplitude of the transmitted EM wave decreases as the plasma slab width increases. Thus the effective EM wave penetration region in the parameter domain of $\tilde{\omega}_{pe0}(\equiv \tilde{n}_0^{1/2})$ and $\tilde{\nu}_{en}$, for the thinner plasma slab, is much larger than that for the wider plasma slab.

(2) In the weak collision regime, the EM wave amplitude A_{EM} falls rapidly when the plasma density goes beyond the level of the critical density ($n_e > n_c$). Nevertheless in the strong collision regime, the amplitude of the EM wave decreases gradually as the normalized plasma frequency (i.e., the square root of the normalized plasma density) increases, and the amplitude of A_{EM} is substantial even if for $n_e > n_c$ ($\omega_{pe} > \omega_0$).

(3) As the collision gets stronger, the wave amplitude A_{EM} varies monotonously in the dense regime ($\tilde{\omega}_{pe0} > 1$, $n_0 > n_c$), but nonmonotonously in the low density regime ($\tilde{\omega}_{pe0} < 1$, $n_0 < n_c$).

(4) For various density profiles, we find that if the maximum plasma number density (n_0) is equal to n_c, the maximum reflection/absorption is located at the critical point; if the maximum plasma number density (n_0) is higher than n_c, the maximum reflection/absorption is moved to a higher density spot between the critical point and where the plasma number density just reaches n_0.

The results outline the propagation characteristics of EM waves in the plasma slabs, and show a successful application of the model and the differential thin layer method developed in this paper. The model and the method can also be generalized and applied for further study on the EM wave propagation in different kinds of geometry structure of the plasmas.

ACKNOWLEDGMENT

This work has been supported by the National Natural Science Foundation of China (No. 11405038), the Fundamental Research Funds for the Central Universities (Grant No. HIT.NIRIF. 201663), and the China Postdoctoral Science Foundation funded project (2015M570283).

[1] V. A. Rozhansky and L. D. Tsendin, *Transport phenomenon in partially ionized plasma* (Taylor and Francis, London, 2001).
[2] T. E. Magin and G. Degrez, J. Comput. Phys. **198**, 424 (2004).
[3] H. M. Gao and P. T. Fa, Chinese Phys. Lett. **25**, 2562 (2008).
[4] W. Daughton, P. J. Catto, B. Coppi, and S. I. Krasheninnikov, Phys. Plasmas **5**, 2217 (1998).
[5] Z.-B. Wang and Q.-Y. Nie, AIP Advances **5**, 097123 (2015).
[6] B. Guo and X.-G. Wang, Phys. Plasmas **12**, 084506 (2005).
[7] L. Zheng, Q. Zhao, S.-Z. Liu, X-J. Xing, and Y.-X. Chen, J. Infrared Millim. Te. **35**, 187 (2014).
[8] P. K. Shukla and G. Morfill, Phys. Lett. A **216**, 153 (1996).
[9] R. Marqués, J. Martel, F. Mesa, and F. Medina, Phys. Rev. Lett. **89**, 183901 (2002).
[10] Z.-Q. Chen, M.-H. Liu, L. Tang, P. Hu, and X.-W. Hu, J. Appl. Phys. **106**, 013314 (2009).
[11] T. C. Lin and L. K. Sproul, Comput. Fluids **35**, 703 (2006).

[12] M. Laroussi, Int. J. Infrared Milli. **17**, 2215 (1996).
[13] J. T. Li and L. X. Guo, J. Electromagnet. Wave **26**, 1767 (2012).
[14] C. T. Swift and J. S. Evans, *Generalized treatment of plasma electromagnetic waves passing through an isotropic inhomogeneous plasma slab at arbitrary angles of incidence* (NASA Report, Washington, 1963).
[15] D. J. Gregoire, J. Santoru, and R. W. Schumacher, *Electromagnetic-wave propagation in unmagnetized plasmas* (AD report, Malibu, 1992).
[16] M. Laroussi, Int. J. Infrared Millim. Waves **17**, 2215 (1996).
[17] M. Laroussi and J. R. Roth, IEEE Trans. Plasma Sci. **21**, 366 (1993).
[18] M. Laroussi, Int. J. Infrared and Millim. Waves **16**, 2069 (1995).
[19] W. L. Barnes, A. Dereux, and T. W. Ebbesen, Nature **424**, 824 (2003).
[20] Y. B. Xi and Y. Liu, Phys. Plasmas **19**, 073301 (2012).
[21] D. K. Kalluri, V. R. Goteti, and A. M. Sessler, IEEE Trans. Plasma Sci. **21**, 70 (1993).
[22] L. J. Xu and N. C. Yuan, IEEE Antenn. Wirel. Pr. **5**, 335 (2006).
[23] Z. H. Qian, R. S. Chen, H. W. Yang, K. W. Leung, and E. K. N. Yung, Microw. Opt. Techn. Let. **47**, 147 (2005).
[24] Z. H. Qian, R. S. Chen, K. W. Leung, and H. W. Yang, Prog. Electromagn. Res. **52**, 173 (2005).
[25] B. Guo, X. G. Wang, and Y. Zhang, Plasma Sci. Technol. **8**, 558 (2006).
[26] X.-T. Gao, C.-S. Wang, B.-H. Jiang, and Z.-L. Zhang, Phys. Plasmas **21**, 093301 (2014).